Clinical Science (2020) **134** 2565–2580
https://doi.org/10.1042/CS20200973

Research Article

Small intestine resection increases oxalate and citrate transporter expression and calcium oxalate crystal formation in rat hyperoxaluric kidneys

Yi-Shiou Tseng[1,2], Wen-Bin Wu[3], Yun Chen[4], Feili Lo Yang[5] and Ming-Chieh Ma[3]

[1]Division of Urology, Department of Surgery, Far Eastern Memorial Hospital, New Taipei, Taiwan; [2]Ph.D. Program in Nutrition and Food Science, Fu Jen Catholic University, New Taipei, Taiwan; [3]School of Medicine, Fu Jen Catholic University, New Taipei, Taiwan; [4]Division of Pediatric Surgery, Department of Surgery, Far Eastern Memorial Hospital, New Taipei, Taiwan; [5]Department of Nutritional Science, Fu Jen Catholic University, New Taipei, Taiwan

Correspondence: Ming-Chieh Ma (med0041@mail.fju.edu.tw)

Short bowel (SB) increases the risk of kidney stones. However, the underlying mechanism is unclear. Here, we examined how SB affected renal oxalate and citrate handlings for *in vivo* hyperoxaluric rats and *in vitro* tubular cells. SB was induced by small intestine resection in male Wistar rats. Sham-operated controls had no resection. After 7 days of recovery, the rats were divided into control, SB (both fed with distilled water), ethylene glycol (EG), and SB+EG (both fed with 0.75% EG for hyperoxaluric induction) groups for 28 days. We collected the plasma, 24 h of urine, kidney, and intestine tissues for analysis. Hypocitraturia was found and persisted up to 28 days for the SB group. Hypocalcemia and high plasma parathyroid hormone (PTH) levels were found in the 28-day SB rats. SB aggravated EG-mediated oxalate nephropathy by fostering hyperoxaluria and hypocitraturia, and increasing the degree of supersaturation and calcium oxalate (CaOx) crystal deposition. These effects were associated with renal up-regulations of the oxalate transporter solute carrier family 26 (Slc26)a6 and citrate transporter sodium-dependent dicarboxylate cotransporter-1 (NaDC-1) but not Slc26a2. The effects of PTH on the SB kidneys were then examined in NRK-52E tubular cells. Recombinant PTH attenuated oxalate-mediated cell injury and up-regulated NaDC-1 via protein kinase A (PKA) activation. PTH, however, showed no additive effects on oxalate-induced Slc26a6 and NaDC-1 up-regulation. Together, these results demonstrated that renal NaDC-1 upregulation-induced hypocitraturia weakened the defense against Slc26a6-mediated hyperoxaluria in SB kidneys for excess CaOx crystal formation. Increased tubular NaDC-1 expression caused by SB relied on PTH.

Introduction

Patients who have undergone bowel resection often have kidney stones. The short bowel (SB) patients had a largely increased incidence of calcium oxalate (CaOx) kidney stones 8–10 years after small intestine resection [1,2]. Low urine volume and pH, hyperoxaluria, and hypocitraturia are known to be the risk factors for patients with SB surgery who develop kidney stone formation [2]. These factors were attributed as a result of intestinal dysfunction after resection. It, however, is unclear whether there is a renal mechanism involved in these changes.

Abnormal oxalate handling usually leads to CaOx stones, which is the most common type of kidney stone. Oxalate can be eliminated by intestinal and renal clearances after dietary intake or endogenous synthesis from liver. Oxalate is secreted actively by the anion transporter solute carrier family 26 (Slc26)

Received: 28 July 2020
Revised: 29 September 2020
Accepted: 02 October 2020

Accepted Manuscript Online: 02 October 2020
Version of Record published: 13 October 2020

Clinical Science (2020) **134** 2565–2580
https://doi.org/10.1042/CS20200973

protein in intestinal epithelium and renal tubular cells. Two members of this family, Slc26a2 and Slc26a6, are present in both intestine and kidney and contribute to different degrees of oxalate exchange activity with other anions [3,4]. In the Slc26a6 null mice, the most striking phenotype was hyperoxaluria-mediated CaOx urolithiasis, which was caused by defective intestinal secretion of ingested oxalate [3]. In SB syndrome, unabsorbed fats bind to Ca^{2+} and leave the increased oxalate to be absorbed from the colon as a result of hyperoxlauria and CaOx stone formation [5]. Nephrolithiasis in SB is known to be prevented by maintaining the patient on a low oxalate diet [6]. Moreover, oxalate is toxic to renal tubular cells [7]. The cell debris of injured tubular cells favors CaOx crystal formation as a seed in crystal growth and aggregation other than hyperoxaluria.

Apart from hyperoxaluria, SB also decreased the intestinal absorption and therefore diminished the urinary excretion of citrate as a result of hypocitraturia in patients [2]. Citrate normally acted as an inhibitor of CaOx crystallization, which had a higher affinity for Ca^{2+} than oxalate and reduced free Ca^{2+} in the urine to prevent supersaturation in stone formation [8,9]. In addition, citrate also adhered to the formed crystal surface to reduce crystal growth and attach to the epithelia [10]. The sodium-dependent dicarboxylate cotransporter-1 (NaDC-1) is the primary citrate transporter, most of which are distributed in the intestine and the proximal tubule of the kidneys [11]. We previously showed enhanced renal NaDC-1 expression in the hyperoxaluric rats and this contributed to hypocitraturia with a loss of the anticrystallization defense against CaOx crystal formation [12]. A previous study showed that NaDC-1 reciprocally regulated Slc26a6 activity as Slc26a6 inhibited NaDC-1, and NaDC-1 activated Slc26a6 for citrate reabsorption and oxalate secretion, respectively [13]. The destruction of this function likely leads to CaOx formation.

Researchers developed an experimental platform in the rat model of SB that mimics human kidney stone formation after SB resection or bypass [14]. In that study, resected rats fed with high oxalate and lipids presented higher hyperoxaluria than rats without resection [14]. They found that crystal formation was not related to urinary supersaturation and suggested that oxalate transporters induced local saturation inside the kidney, which may be responsible for crystal deposition [14]. This raises an interesting question regarding whether enhanced oxalate secretion via its transporter boosts CaOx crystal formation as a renal mechanism in SB rats when challenged with hyperoxaluria. This issue, however, is not yet tested. We, therefore, hypothesized that inappropriate renal handling of oxalate and citrate may contribute to CaOx crystal formation in SB kidneys. The present study used ethylene glycol (EG) as a precursor of oxalate to induce hyperoxaluria and CaOx crystal formation in male Wistar rats and to assess the *in vivo* effects of SB. Changes in oxalate and citrate transporter expressions in the intestines and the kidneys were examined to see how SB affects oxalate and citrate handling. In order to gain insight into the SB effects, we examined the cellular mechanism of changes in oxalate and citrate transporter expressions in renal tubular cells *in vitro*.

Materials and methods

Experimental animals and study designs

Male Wistar rats (BioLASCO, the authorized distributor for Charles River Laboratories in Taipei, Taiwan) weighing approximately 200–250 g were used in the present study as experimental animals. A total of four groups included six rats in each group, and the experimental period was 28 days. The control group received the sham operation as described below. Distilled water was given as drinking water for the control (C) group. The ethylene glycol (EG) group received a sham operation and was fed with 0.75% of EG in the drinking water. The SB group received an 80% small intestine resection as described below and was fed with distilled water. The SB+EG group received an 80% resection and were fed with 0.75% of EG. All rats had free access to food and consumed standard chow. Drinking water was limited to 40 ml per day for each rat. The rats were housed in metabolic cages on days 1 and 28 for a 24-h collection of urine, feces, and monitoring their food intake.

After 28 days, the rats were anesthetized using sodium pentobarbital (65 mg/kg, intraperitoneal) for the collection of arterial blood and killed to harvest the kidneys and colons after transcardiac perfusion [12]. The kidneys were sliced and kept in 10% formalin for CaOx crystal analysis. The renal tissues and colons were kept at −80°C for further biochemical examination. All animal experiments were performed at the Far Eastern Memorial Hospital in compliance with the Guide for the Care and Use of Laboratory Animals (published by National Academy Press, Washington DC, 2011) and were reviewed and approved by the Institutional Animal Care and Use Committee of Far Eastern Memorial Hospital (IACUC-2018-FEMH-08) in Taiwan.

Surgical procedure of small intestine resection

The rats were anesthetized using sodium pentobarbital sodium (65 mg/kg, intraperitoneal). The rats were then placed on a servo-null heating plate to maintain their body temperature at ∼37°C via a rectal thermometer. As shown in Figure 1, the abdomen was opened under disinfection. The duodenum, small intestine, and cecum were all exposed

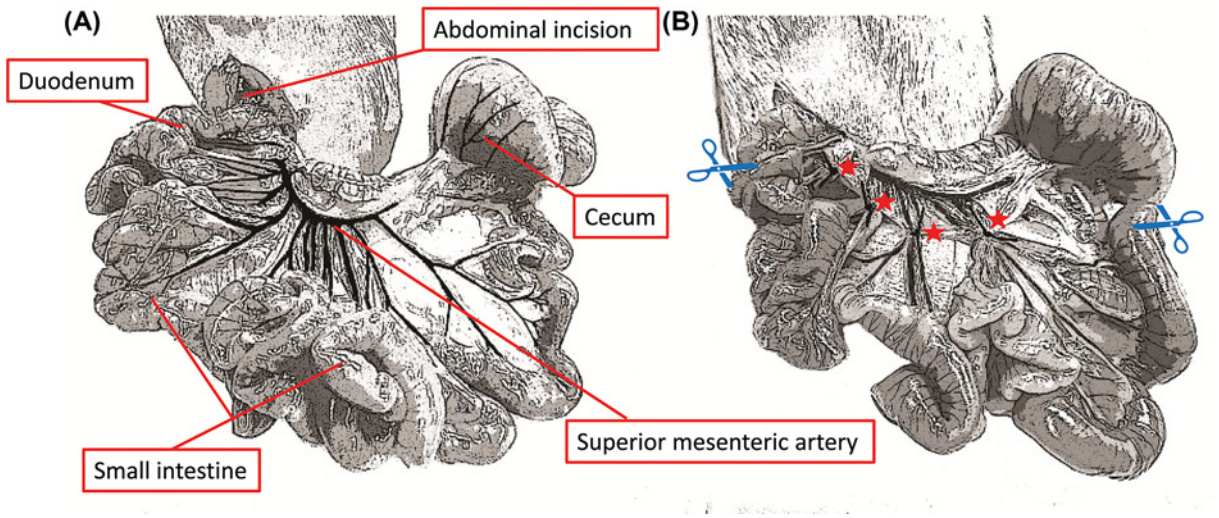

Figure 1. Anatomic diagram of the small intestine resection in SB rats

(**A**) The duodenum, small intestine, and cecum were exposed from the abdominal cavity under aseptic conditions after the abdomen was opened. (**B**) Four star signs (red) indicate the ligation of the vascular branches of the superior mesenteric artery, which were cut distal during the resection. Two scissor signs (blue) indicate the resection sites of the small intestine for further anastomosis.

to the abdominal cavity. To avoid resected tissue bleeding, the branches of the superior mesenteric artery were ligated as indicated in Figure 1. Approximately 80% of the small intestine was removed between the duodenum and cecum. Electrocautery was used to stop the bleeding during the resection with minimal blood loss. The residual intestine and cecum were anastomosed with a 6-0 prolene suture, and the abdominal wall was sutured. A sham operation was performed with abdominal opening and exposure of the gastrointestinal tract but without resection. After surgery, the rats were placed in individual cages and warmed by a heat lamp to avoid body temperature loss. Distilled water containing 5% glucose was supplied for 1 day after surgery and standard chow was given 24 h after surgery. The mortality rate of SB rats was 20% (3/15). Two of them died because of intra-abdominal bleeding, the third rat was killed because of malnutrition by loss of more than 20% of body weight after 4 days of surgery.

Plasma chemistry and urinalysis

The blood and 24-h urine samples were then centrifuged and the supernatant was sampled for the following biochemical analyses. The urinary pH was measured using a standard pH meter. The concentration of Ca^{2+} in the plasma and urine were measured using an electrolyte analyzer (Dri-Chem 3500i, Fuji, Tokyo, Japan) as described previously [12]. The plasma parathyroid hormone (PTH) levels were determined using a commercial kit (RayBiotech, Norcross, GA) following the manufacturer's instructions. The oxalate and creatinine levels in the plasma and urine were determined using commercial kits (Trinity Biotech Plc, Bray, Co. Wicklow, Ireland; BioQuant, Reinach, Switzerland, respectively) as described previously [12]. Creatinine clearance (Ccr) was then calculated accordingly. The urinary magnesium and citrate levels were determined using commercial kits (BioAssay Systems, Hayward, CA, U.S.A.; r-Biopharm, Woodfield Boulevard, Caringbah, Australia, respectively) as described previously [12]. Urinary lactate dehydrogenase (LDH, a marker of tubular damage) was measured using a commercial kit (Roche Applied Science, IN, U.S.A.) as described previously [18]. The degree of urine supersaturation was calculated according to the formula of the ion activity product of calcium oxalate (AP(CaOx) index; $4076 \times \text{calcium}^{0.9} \times \text{oxalate}^{0.96})/((\text{citrate} + 0.015)^{0.60} \times \text{magnesium}^{0.55} \times \text{urine volume}^{0.99})$ as described previously [15].

Detection of CaOx crystals in rat kidneys

The kidney tissue was sectioned into 5-μm-thickness and Pizzolato's staining was applied to recognize the presence of CaOx crystals as described previously [16]. In brief, a mixed solution of equal quantities of 5% silver nitrate and 30% hydrogen peroxide was applied to slides to cover the tissue sections. The slides were exposed to light from a 60-W incandescent lamp at a distance of 15 cm for 30 min. The slides were washed with distilled water, counterstained with nuclear first red solution for 5 min, and dehydrated in 95% alcohol. The black regions were identified as CaOx

Clinical Science (2020) **134** 2565–2580
https://doi.org/10.1042/CS20200973

crystals. The renal section was magnified at 200× under an optical microscope and five images with an area of 100 μm^2 in one section were taken to count and average the crystal numbers.

Tubular cell culture and drug treatment

To examine the effects of PTH on NaDC-1, NRK-52E cells were used because the PTH receptor is known to be present in this cell line as previously reported [17]. The cells were purchased from the Bioresource Collection and Research Center (Hsinchu, Taiwan). This cell line was originally derived from the American Type Culture Collection lines, CRL-1571. All culture medium and supplements were purchased from Thermo Scientific HyClone (South Logan, UT, U.S.A.). The cells were grown in Dulbecco's modified Eagle's medium with 5% fetal bovine serum, 100 U/ml penicillin, and 100 μg/ml streptomycin, in 5% CO_2 at 37°C. The cells were maintained and subcultured every 3 days when they reached confluence. The cells were seeded in a six-well plate for 2 days. On the day of experiment, 100 μl of culture medium of each well was sampled and mixed with chemicals to achieve the final concentration as below. The cells were treated with phosphate-buffered saline (as control, pH 7.4), oxalate (Oxa, 0.5 mM, Sigma–Aldrich, St. Louis, MO, U.S.A.), recombinant PTH (1-34) (0.1 μM, Sigma–Aldrich), selective protein kinase A (PKA) inhibitor H89 (0.5 μM, Sigma–Aldrich), or KT5720 (1 μM, Sigma–Aldrich) alone or in combination for 48 h. The doses for PKA blockers were chosen based on their IC_{50} values.

Cell viability and assays

We used a commercial kit to measure the levels of LDH (Roche Applied Science, IN, U.S.A.) in the cell culture medium to evaluate cell damage as described previously [18]. MTT (3-(4,5-dimethylthiazol-2-yl)-2,5-diphenyltetrazolium bromide, Sigma–Aldrich) assay was used to measure the cell viability. Briefly, the medium was removed and the cells were washed three times with phosphate buffered saline (PBS, pH 7.4) after 48 h. MTT (0.5 mg/ml in PBS) was then added to cells and incubated for 4 h at 37°C. MTT formazan crystals were then dissolved in dimethyl sulfoxide and we measured the optical density (O.D.) with an enzyme-linked immunosorbent assay plate reader (Amersham-Pharmacia Biotech, Piscataway, NJ, U.S.A.) at 570 nm. The cell viability (%) was calculated using the following formula:

$$\left(\frac{\text{O.D. of treated sample}}{\text{O.D. of control sample}}\right) \times 100$$

Western blot analysis for protein expression

We examined the expressions of Slc26a2, Slc26a6, NaDC-1, and β-actin by immunoblot analysis in the cultured cells and kidney tissue, as described previously [12]. Primary antibodies against the above proteins were obtained from Santa Cruz Biotechnology (Santa Cruz, CA, U.S.A.) for Slc26a6, NaDC-1, and β-actin, and from Abcam (Cambridge, U.K.) for Slc26a2. Briefly, equal amounts of total protein were separated in denaturing sodium dodecyl sulfate/polyacrylamide gels and electrophoretically transferred to polyvinylidene difluoride membranes (Amersham-Pharmacia Biotech, Little Chalfont, U.K.). The membranes were then incubated with the appropriate primary antibody (1:1000 for Slc26a2 and Slc26a6; 1:500 for NaDC-1; and 1:2000 for β-actin) overnight at 4°C. After washing, the membranes were incubated for 1 h at room temperature with the corresponding horseradish peroxidase-conjugated secondary antibodies (1: 200; Vector Laboratories, Burlingame, CA, U.S.A.). The bound antibodies were visualized using an enhanced chemiluminescence kit (Amersham-Pharmacia Biotech) and Kodak film. The band density was measured semi-quantitatively using an image analysis system (Diagnostic Instruments, Sterling Heights, MI, U.S.A.). The amount of each protein was expressed relative to the amount of actin.

Statistics

Numerical data are presented as the mean ± the standard error of the mean (S.E.M). We conducted our statistical analysis using Prism 3.0 for Windows software (GraphPad Software Inc, San Diego, CA, U.S.A.). The differences between subgroups were analyzed using an unpaired *t* test or one-way ANOVA. Differences were regarded as significant at $P<0.05$.

Results

Basic health parameters before hyperoxaluric induction

Before hyperoxaluric induction, SB rats ($n=12$) showed similar body weight, daily food intake, urine output and pH, and feces when compared with those in the Sham rats ($n=12$) after 7 days of recovery from surgery (Table 1). SB

Table 1 Basic health parameters of rats before hyperoxaluric induction

Index/groups	Sham	SB
Body weight (g)	233.6 ± 3.4	229.1 ± 5.3
Food intake (g)	27.1 ± 1.1	23.9 ± 3.1
Urine amount (ml/day)	27.7 ± 2.3	24.7 ± 4.2
Feces (g/day)	12.6 ± 0.9	13.0 ± 1.5
Urine pH	8.1 ± 0.2	8.1 ± 0.2
Urine Ca^{2+} (mg/day)	0.40 ± 0.05	0.23 ± 0.02*
Urine oxalate (mg/day)	3.0 ± 0.9	2.4 ± 0.8
Urine citrate (mg/day)	3.1 ± 0.2	1.2 ± 0.1*

The data were obtained from a metabolic cage study collected over a 24-h period after the rats treated with a sham operation (Sham) or SB resection (SB) for 7 days. Hypocalciuria and hypocitraturia were noticed in SB rats when compared with the Sham rats. n=12 in each treatment.
*P<0.05, SB vs. Sham rats.

significantly decreased the daily urine excretion of Ca^{2+} and citrate when compared with the Sham rats. A power analysis showed that the sample size of 12 in Table 1 has an 80% power to detect an effect size as a Cohen's d greater than 0.8 unit assuming a 5% significance level.

Effects of SB and EG on basic health parameters for 28 days of treatment

After 28 days of hyperoxaluric induction, the gain of body weight was similar among four subgroups (n=6 in each, Figure 2A). There was no statistical difference in the amount of daily food intake, urine output, and feces after 28 days (Figure 2B–D). The ratio of the kidney weight to body weight (KW/BW) increased significantly in the SB+EG group (1.3 ± 0.1%) when compared with the SB (1.1 ± 0.1%) or EG (1.1 ± 0.1%) group (Figure 2E).

Changes in plasma levels of Ca^{2+}, citrate, oxalate, and PTH

The plasma Ca^{2+} levels were lowered in the SB (8.6 ± 0.2 mM) and SB+EG (8.6 ± 0.1 mM) groups when compared with their corresponding control groups (9.6 ± 0.2 and 9.3 ± 0.2 mM in the C and EG groups, respectively) with a similar degree of hypocalcemia (Figure 3A). There was a slight increase in the plasma oxalate in the EG group; however, this was insignificant when compared with the control group (Figure 3B). The SB or SB+EG groups showed no effect on the plasma oxalate level. The plasma citrate levels were similar among groups although insignificant low levels were found in the SB group (Figure 3C). The plasma PTH levels were significantly increased in both the SB (36.6 ± 5.1 pg/ml) and SB+EG (42.7 ± 5.5 pg/ml) groups when compared with their corresponding control groups (22.1 ± 2.1 and 26.4 ± 2.6 pg/ml in the C and EG groups, respectively) (Figure 3D).

Effects of SB and EG on urinary chemistry

The urinary pH 7.1 ± 0.1 was lowered in the EG group; a similar low urinary pH 7.0 ± 0.3 was also found in the SB+EG group when compared with 8.0 ± 0.1 in the control group and 7.7 ± 0.3 in the EG group, respectively (Figure 4A). The urinary Ca^{2+} excretion was similar among groups (Figure 4B). Hyperoxaluria was successfully induced in both EG groups (Figure 4C). SB alone did not affect the oxalate excretion but did significantly augment the severity of hyperoxaluria in the SB+EG group (39.4 ± 3.9 mg/day) when compared with the EG group (18.6 ± 1.5 mg/day). EG lowered the urinary citrate level (Figure 4D); this was similar to our previous finding [12]. SB also induced hypocitraturia and augmented EG-induced hypocitraturia in the SB+EG group. Ccr was similar among groups, indicating these treatments did not affect renal function after 28 days (Figure 4E). Because tubular damage aggregates CaOx crystals, we next tested whether SB may affect tubular damage in the EG kidney. Using a reliable marker of tubular damage, our results showed that urinary excretion of LDH in the EG group (6.4 ± 0.8 units/day) increased significantly compared with that in the control group (1.3 ± 0.5 units/day) (Figure 4F). SB itself had no effect on LDH excretion (2.1 ± 0.7 units/day), but markedly aggravated LDH excretion in the SB+EG group (10.6 ± 1.5 units/day). In calculating the AP(CaOx) index to estimate the degree of supersaturation, both EG groups had higher AP(CaOx) index than their corresponding control groups (Figure 4G). The increased AP(CaOx) index, however, was more prominent in the SB+EG group (125 ± 48 units) when compared with the SB (6 ± 3 units) or EG (50 ± 11 units) group.

Clinical Science (2020) **134** 2565–2580
https://doi.org/10.1042/CS20200973

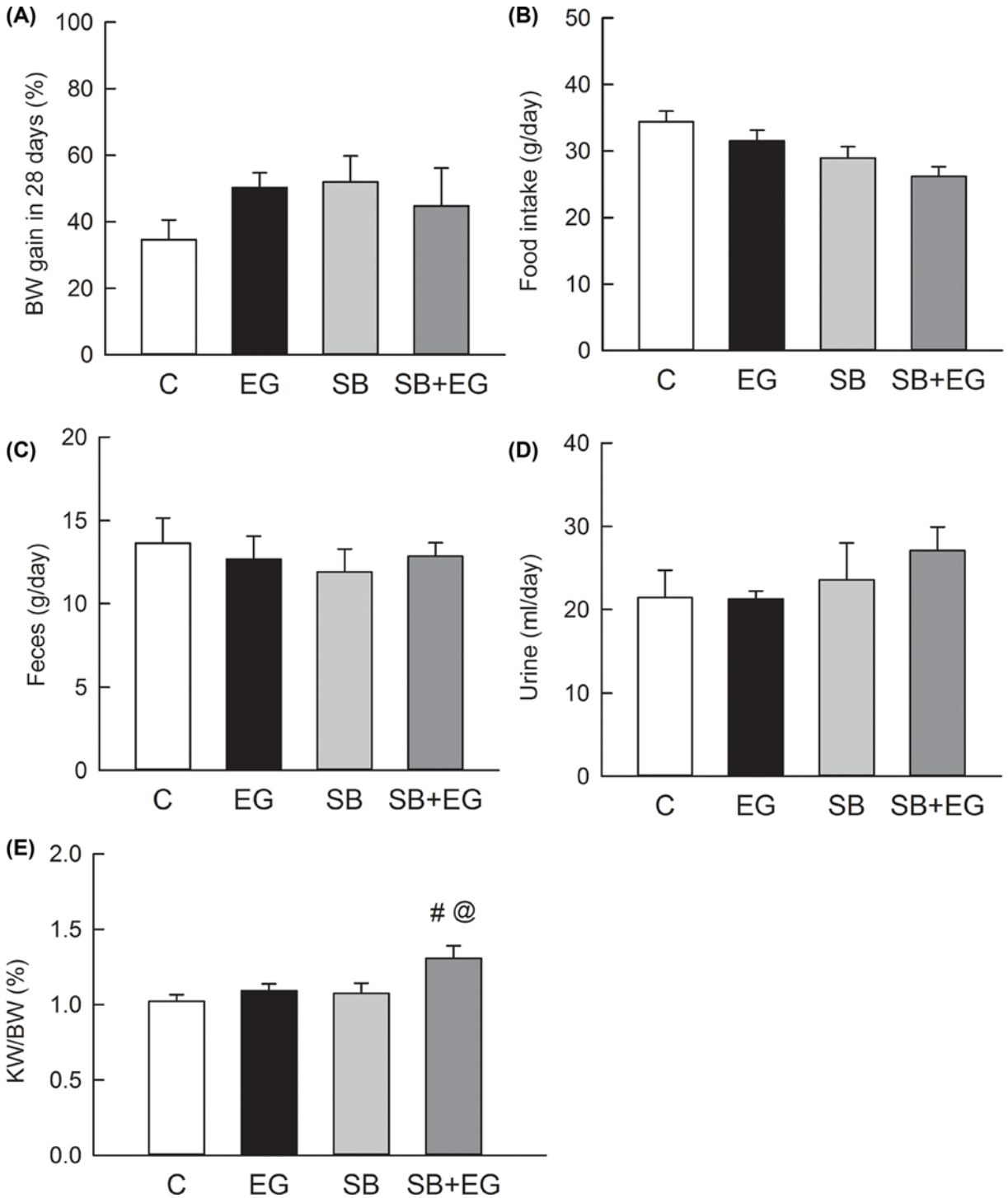

Figure 2. Basic health parameters after 28 days of treatment

The data were obtained from a metabolic cage study collected over a 24-h period after 28 days of induction of body weight (BW) gain (**A**), daily food intake (**B**), feces amount (**C**), urine output (**D**), and kidney weight (KW) to BW ratio (**E**). A significant increase in the KW/BW ratio was found in the SB+EG group when compared with the EG or SB group. n=6 in each group. C, control; EG, ethylene glycol (hyperoxaluria); SB, small intestine resection; SB+EG, small intestine resection co-treated with ethylene glycol. $^{\#}P<0.05$, SB+EG vs. EG group; $^{@}P<0.05$, SB+EG vs. SB group.

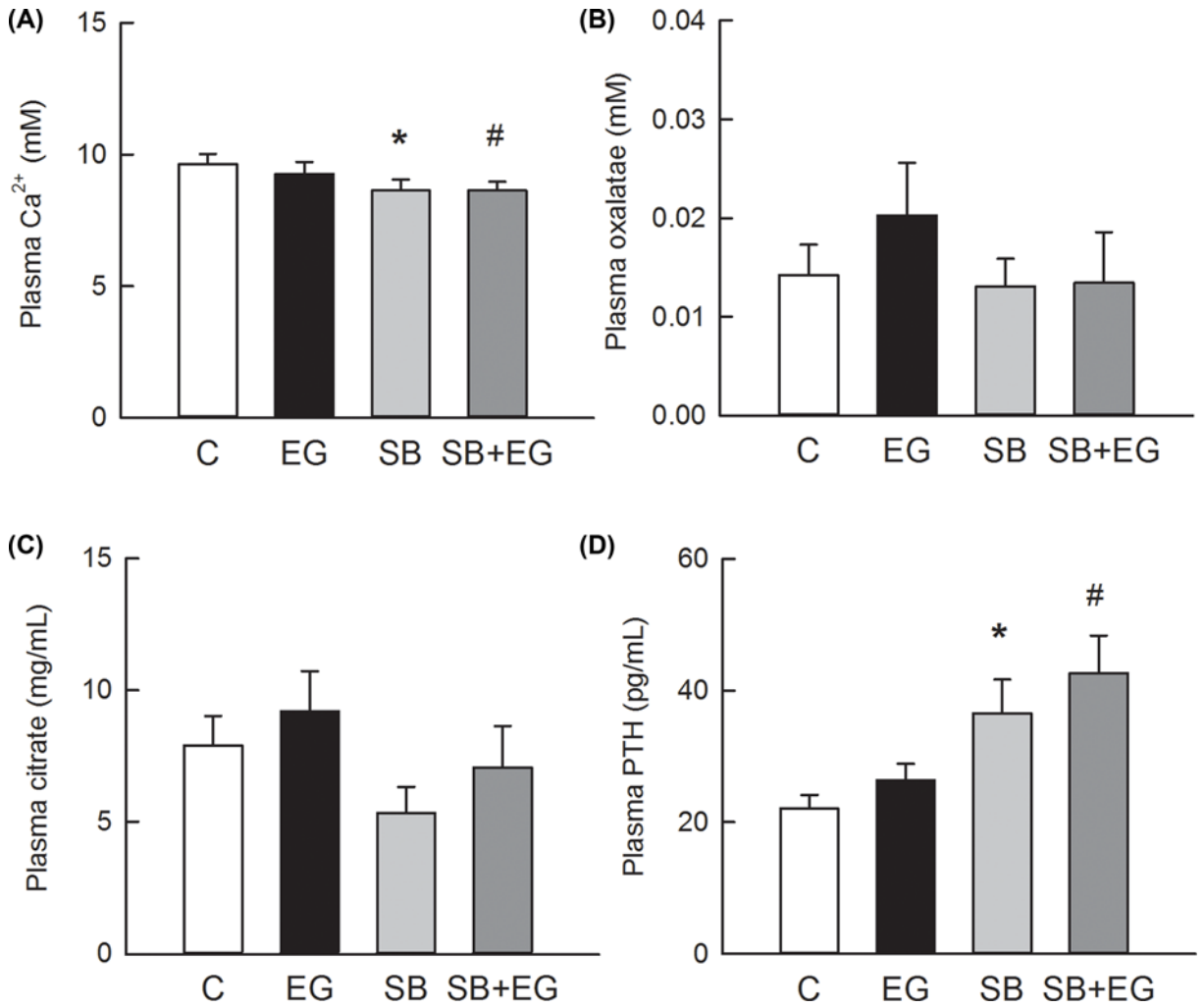

Figure 3. Changes in the plasma biochemistry and PTH levels

The blood was collected from the inferior vena cava after 28 days of treatment for determining the plasma levels of Ca^{2+} (**A**), oxalate (**B**), citrate (**C**), and PTH (**D**). The plasma levels of oxalate and citrate were similar among groups. Hypocalcemia and increases in the plasma PTH were found in both SB-treated groups. n=6 in each group. The group abbreviations are the same as in Figure 2. $^{*}P<0.05$, SB vs. C group; $^{\#}P<0.05$, SB+EG vs. EG group.

Renal CaOx crystal deposition

Using Pizzolato's staining, we found that there was no Ca^{2+} crystal deposition in the kidneys of the control and SB groups (the left two pictures in Figure 5A). Ca^{2+} crystals were found in the hyperoxaluric kidneys of the EG group and this deposition caused tubular lumen dilation (the right upper picture in Figure 5A). There was more CaOx crystal deposition in the SB+EG kidney and more tubular dilation, possibly due to severe obstruction (the right lower picture in Figure 5A). Moreover, a mild interstitial fibrosis surrounding the dilated tubule and tubular atrophy were found in the SB+EG kidney. The number of crystals per area was significantly increased in the EG group (582 $\pm$ 21), and this was aggravated in the SB+EG group (948 $\pm$ 124) (Figure 5B).

Changes in oxalate and citrate transporter expression in the kidneys and intestines

The severe hyperoxaluria and hypocitraturia seen in the SB+EG rats were possibly a result of impaired oxalate and citrate handling in the kidneys and intestines. We, therefore, examined the changes in oxalate and citrate transporter expression in both tissues. The renal expressions of Slc26a6, but not Slc26a2, in the EG and SB+EG groups were significantly increased when compared with those in their corresponding control groups (Figure 6A,B). SB alone showed

Clinical Science (2020) **134** 2565–2580
https://doi.org/10.1042/CS20200973

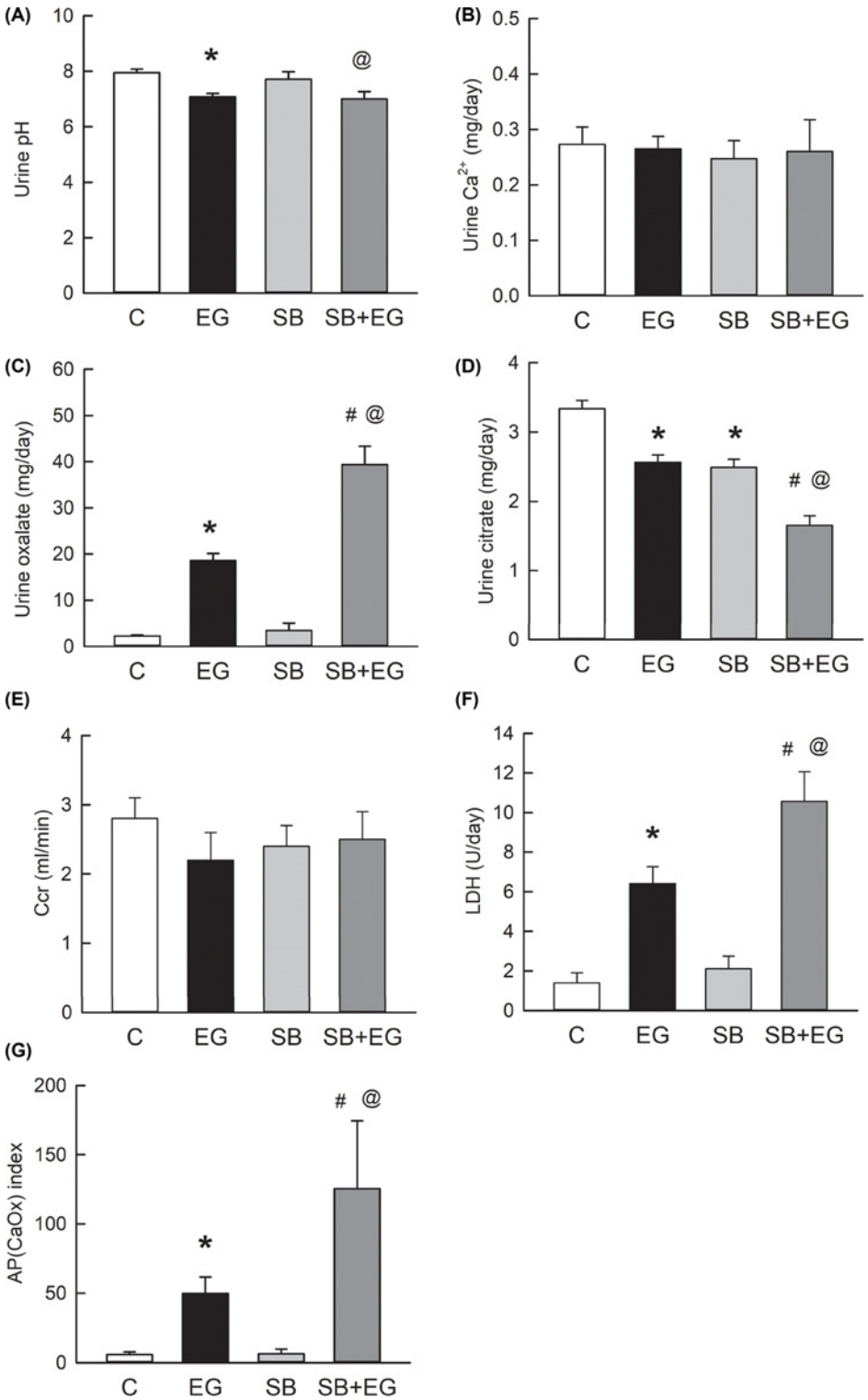

Figure 4. Urinalysis and CaOx supersaturation

Urine was collected from metabolic cages over a 24-h period after 28 days of induction and analyzed for changes in the urinary pH (**A**), Ca^{2+} (**B**), oxalate (**C**), and citrate (**D**) excretion and Ccr, (**E**) and urinary LDH levels (**F**), and the degree of supersaturation as expressed as the AP(CaOx) index (**G**). Low urinary pH was found in both EG-treated rats. Urinary Ca^{2+} excretion and Ccr was similar among groups; these were associated with hyperoxaluria, hypocitraturia, enzymuria, and supersaturation in the SB or EG group with a more prominent change in the SB+EG group. U, units. n=6 in each group. The group abbreviations are the same as in Figure 2. $^{*}P<0.05$, EG or SB vs. C group; $^{\#}P<0.05$, SB+EG vs. EG group; $^{@}P<0.05$, SB+EG vs. SB group.

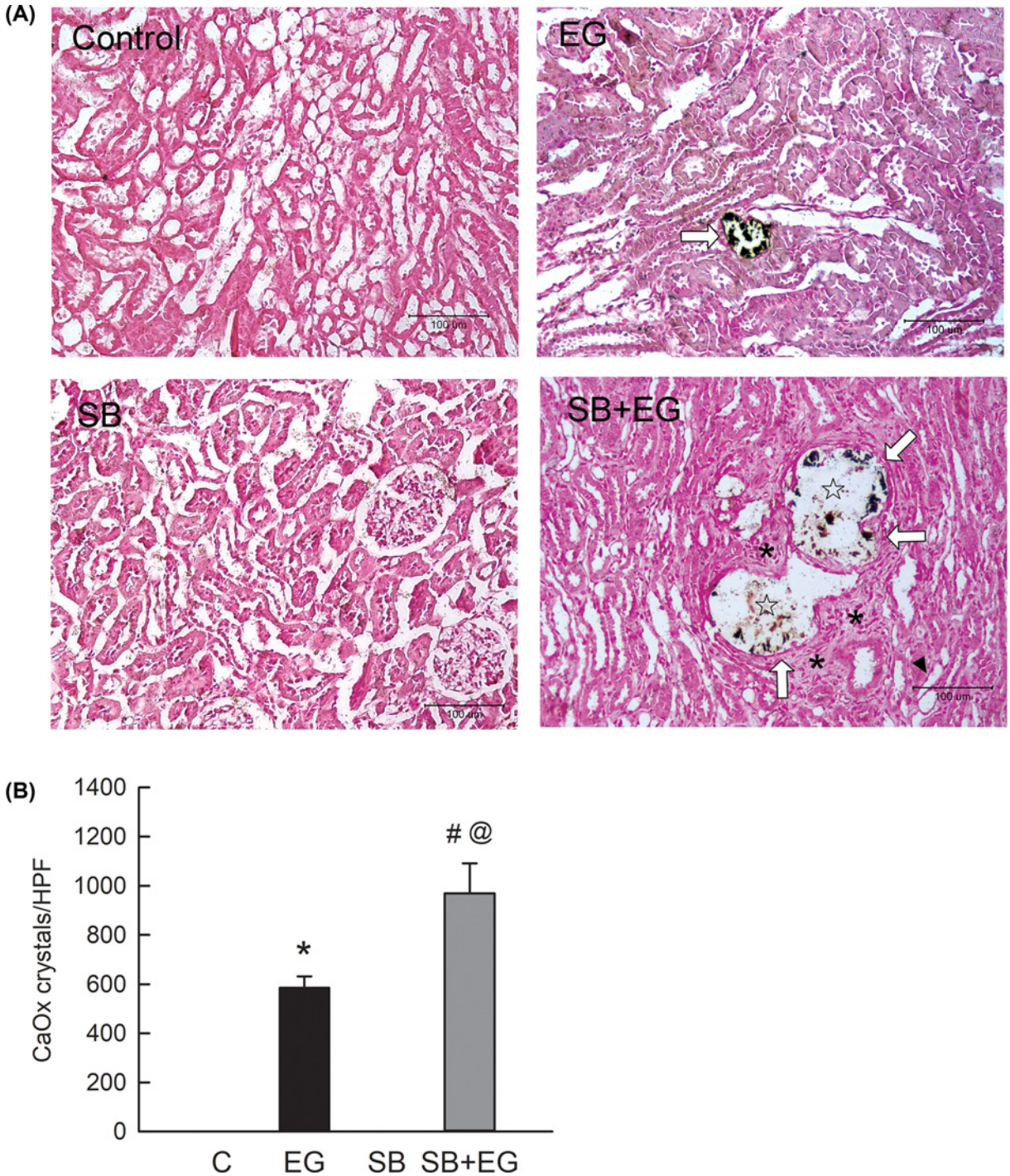

Figure 5. The effects of SB on renal CaOx crystal deposition

Representative micrographs of light microscopy after Pizzolato's staining and counterstaining with Eosin Y in rat kidneys with 28 days of treatment showed CaOx crystal deposition (**A**). CaOx crystal deposition (indicated by open arrows) in the sections. CaOx crystals in the SB+EG kidney led to renal tubular obstruction and dilation (asterisk). A mild interstitial fibrosis (star signs) surrounding the dilated tubule and tubular atrophy (arrow head) were found in the SB+EG kidney. The amount of CaOx crystals in renal sections was counted under high-power field (HPF) (**B**). No crystals were found in the kidneys of the control and SB groups. The group abbreviations are the same as in Figure 2. $^{*}P<0.05$, EG vs. C group; $^{\#}P<0.05$, SB+EG vs. EG group; $^{@}P<0.05$, SB+EG vs. SB group.

Clinical Science (2020) **134** 2565–2580
https://doi.org/10.1042/CS20200973

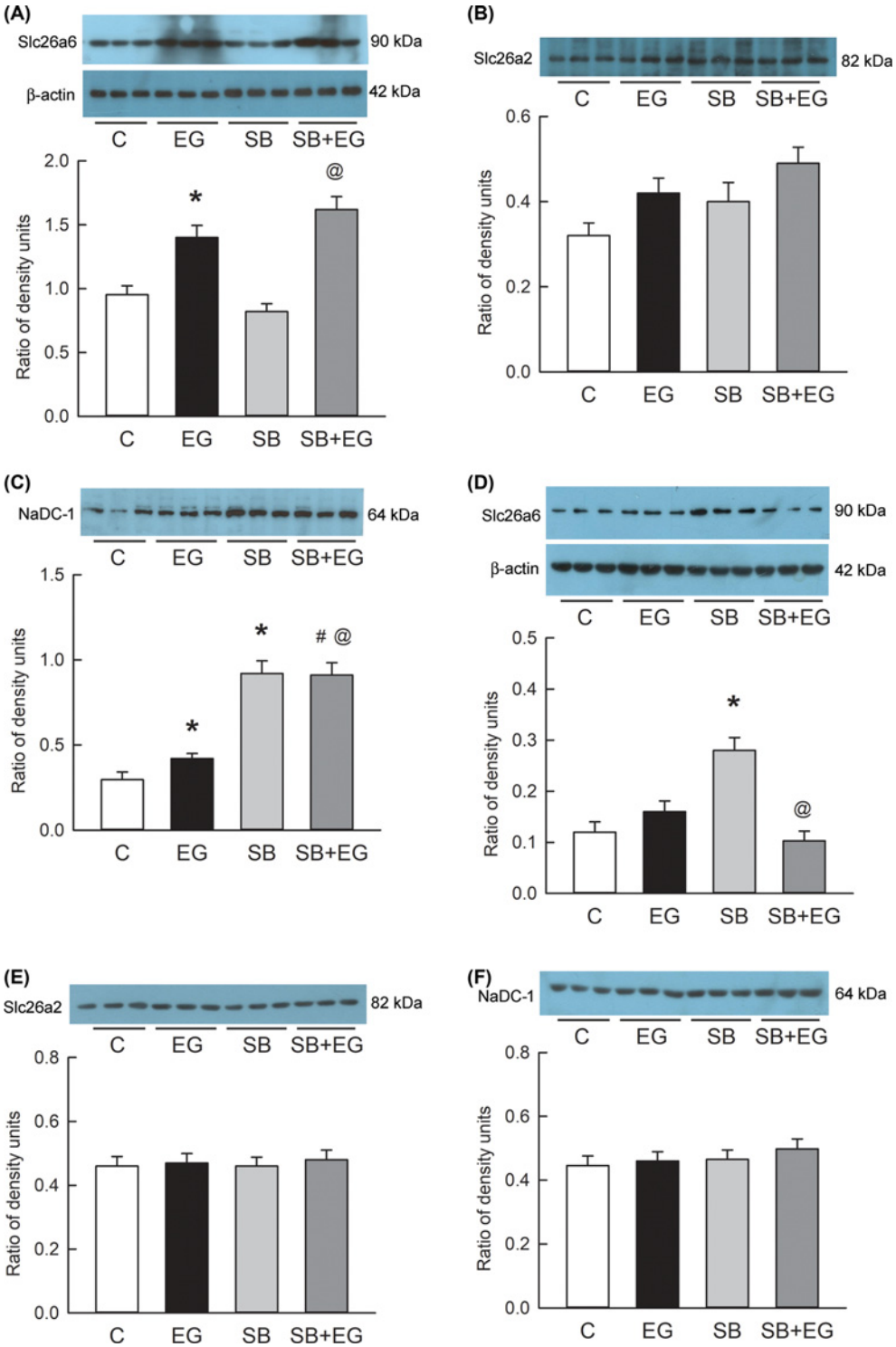

Figure 6. Changes in oxalate and citrate transporter expression

The protein expressions of Slc26a6, Slc26a2, and NaDC-1 in whole kidneys (**A**–**C**) and intestinal (**D**–**F**) tissue extracts were examined by immunoblotting. Representative blots from three rats showed typical protein expression of Slc26a6, Slc26a2, and NaDC-1 (20 μg of total protein per lane) at appropriate molecular weights. The lower bar graph (n=6 in each group) showed the ratio of the band density of the interested protein to β-actin. Slc26a6, but not Slc26a2, was up-regulated in both EG-treated groups; this was associated with increases in the NaDC-1 expression in all experimental groups. The Slc26a6 expression was also increased in the intestines of SB group. The group abbreviations are the same as in Figure 2. $^{*}P<0.05$, SB or EG vs. C group; $^{\#}P<0.05$, SB+EG vs. EG group; $^{@}P<0.05$, SB+EG vs. SB group.

no effect on the renal expression of Slc26a6 and Slc26a2. Compared with the control, EG increased NaDC-1 expression (Figure 6C); this was consistent with our previous findings [12]. NaDC-1 expression was markedly up-regulated in the SB group, this prominent change in the NaDC-1 expression was also found in the SB+EG group. These changes were correlated to hypocitraturia. The intestinal expression of Slc26a6 was significantly increased in the SB group but not in the EG and SB+EG groups when compared with the control group (Figure 6D). The intestinal expressions of Slc26a2 and NaDC-1 were similar among groups (Figure 6E,F).

PTH directly up-regulates NaDC-1 via PKA signaling

As a citricemic hormone, we further tested the effect of PTH in the tubular cells. An increase in LDH release (28.9 $\pm$ 3.1 units/l) and a reduction in cell viability (59 $\pm$ 5%) as tubular cell damage were found in the oxalate (Oxa) group when compared with the control group (7.9 $\pm$ 0.8 units/l in LDH and 100 $\pm$ 6% in cell viability, n=6 in each group, Figure 7A,B), indicating tubular cell damage caused by oxalate. These were attenuated in the PTH+Oxa group (18.9 $\pm$ 1.8 units/l in LDH and 77 $\pm$ 3% in cell viability). No effect on the cell viability, however, was found in the PTH group. The Slc26a6 and NaDC-1 expressions were increased in the Oxa group (Figure 7C,D). The treatment of PTH alone showed no effect on Slc26a6 expression but significantly up-regulated NaDC-1 in the PTH group. The increased Slc26a6 and NaDC-1 expressions in the PTH+Oxa group were similar to those seen in the Oxa and PTH groups, respectively.

The main signaling pathway underlying the PTH receptor is PKA activation [19]. We, thus, examined whether the PKA pathway was involved in changes in Slc26a6 or NaDC-1 expression. Again, Slc26a6 expression was not affected in the PTH group. Two specific blockers of PKA, H89 and KT5720, did not affect Slc26a6 expression in the PTH-treated groups (Figure 7E). The inhibition of PKA activity by the selective blockers H89 and KT5720 significantly attenuated the NaDC-1 up-regulation in the PTH-treated groups (Figure 7F).

Discussion

The present study demonstrated more CaOx crystal deposition in the SB-treated hyperoxaluric kidneys and confirmed previous findings in the rat model and in the SB patients. As in the schematic diagram shown in Figure 8, secondary hyperparathyroidism to enhance PTH release, as a result of hypocalcemia in the SB rats, directly up-regulated the citrate transporter NaDC-1 via the PKA pathway in tubular cells. This possibly contributed to hypocitraturia in the SB rats and would weaken the intrarenal defense mechanisms against CaOx crystal formation. Not only hypocitraturia but also severe hyperoxaluria caused by oxalate transporter Slc26a6 up-regulation after oxalogenic treatment aggravated urinary supersaturation for CaOx crystal formation and deposition in the SB kidneys.

Our results showed that 7-day SB rats demonstrated hypocalciuria (Table 1). While we did not measure plasma Ca^{2+} level at this induction time, it was significantly lowered after 28 days (Figure 3A). Previous studies demonstrated that SB induced steatorrhea with less intestinal Ca^{2+} absorption and insufficient nutrients for the impaired formation of albumin, and these, in turn, lowered the plasma Ca^{2+} concentration [20]. In this study, hypocalciuria was possibly due to intestinal malabsorption, but this was no longer seen after 28 days of SB induction even when there was hypocalcemia (Figures 3A and 4B). Hypocalciuria was associated with normal urine Ca^{2+} excretion and clearly indicated that a deficiency of the Ca^{2+} handling in the SB kidneys was present. We suggest that the hypocalcemia seen in our SB rats was not only dependent on intestinal malabsorption but also relied on impaired renal Ca^{2+} handling.

Hypocalcemia is known as a strong stimulus to the parathyroid gland for PTH release [21]. PTH is not only related to the maintenance of Ca^{2+} homeostasis; a previous study revealed that PTH also acts as a citricemic hormone to maintain the bodily citrate balance [22]. In this study, severe hypocitraturia was found in the SB rats from days 7 to 28 (Table 1 and Figure 4D). This was consistent with clinical observations in SB patients with persistent hypocitraturia [23]. In addition to exogenous resources from the diet, citrate can be synthesized endogenously in mitochondria and enters the tricarboxylic acid cycle for energy production [24].

Energy consideration is important to SB patients who are thought to require a long-term parenteral supplement [25]. SB surgery significantly decreased the available tissues of the intestines for citrate absorption from the diet and left a short passage time for citrate in the remaining intestinal tissues. Plasma citrate is known to be maintained by bone turnover, intestinal absorption, and renal clearance [22]. NaDC-1 is the main transporter responsible for citrate reabsorption with cotransport of Na^+ in the intestines and kidneys [13]. We partially ruled out the bone effects because there was a similar weight gain between the SB and control groups (Table 1 and Figure 2A). Our results showed that intestinal NaDC-1 expression in SB rats was similar to other groups (Figure 6F), indicating there was no compensation for enhancing citrate absorption in the remaining intestinal tissues.

Clinical Science (2020) **134** 2565–2580
https://doi.org/10.1042/CS20200973

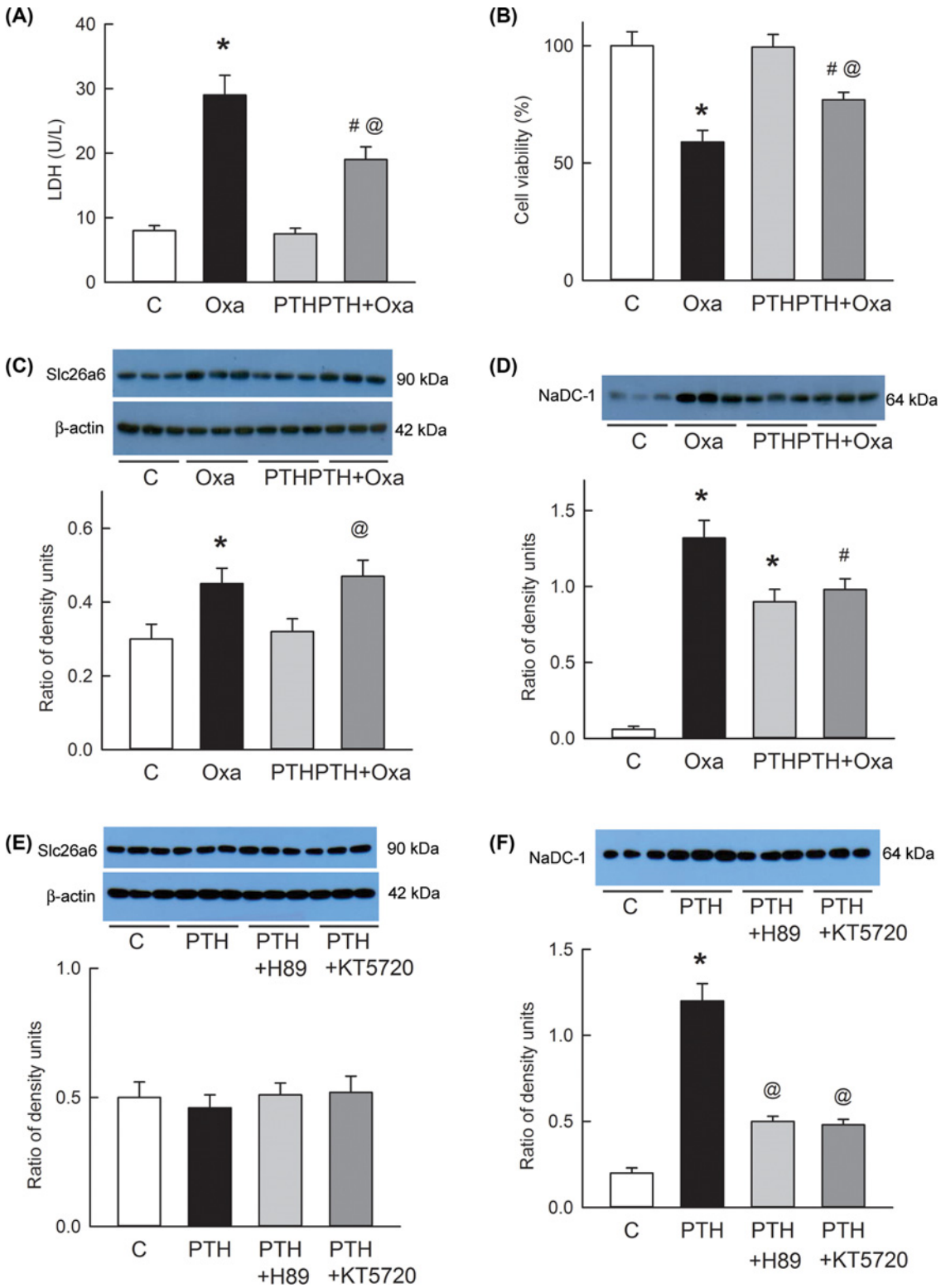

Figure 7. The effects of PTH on oxalate and citrate transporter expression

The responses to Oxa, PTH, and the PKA blockers, H89 and KT5720, were evaluated in NRK-52E cells. (**A**) LDH was released under the treatment of Oxa or PTH alone or in combination. (**B**) The cell viability was examined using the MTT assay. (**C**,**D**) Slc26a6 and NaDC-1 expression in cells treated with oxalate or PTH. (**E**,**F**) Slc26a6 and NaDC-1 expression in cells treated with PTH and PKA blockers, H89 or KT5720. The lower bar graphs (n=6 in each group, C–F) shows the ratio of the band density of the interested protein to β-actin. $^{*}P<0.05$, Oxa or PTH vs. C group; $^{\#}P<0.05$, PTH+Oxa vs. Oxa group; $^{@}P<0.05$, PTH+Oxa vs. PTH group.

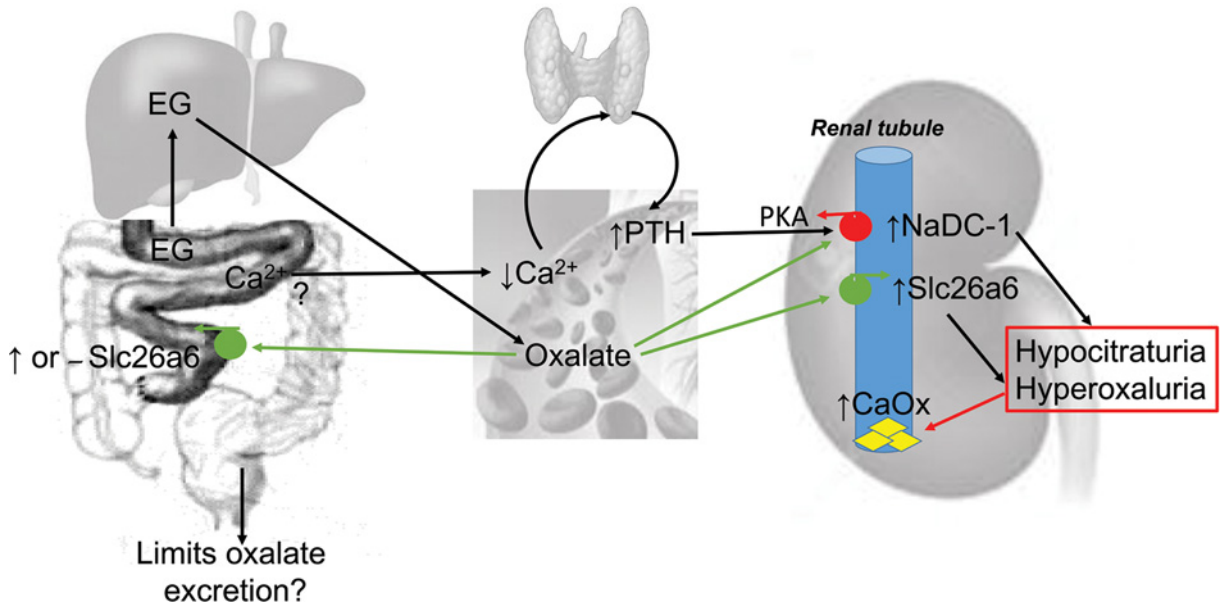

Figure 8. Schematic diagram showing how SB induced hypocitraturia in hyperoxaluric kidneys

SB induced hypocalcemia and PTH release. PTH acted on renal tubules and increased citrate transporter NaDC-1 expression via the PKA pathway, which induced hypocitraturia and lowered the anticrystallization ability of SB kidneys. The oxalogenic treatment of EG increased the Slc26a6 expression in the kidney but not in the intestine of SB rats, aggravating hyperoxaluria for CaOx crystal formation.

Our results further demonstrated that NaDC-1 expression was up-regulated in the SB kidneys (Figure 6C); this likely enhanced the citrate reabsorption by the reduction in renal excretion. Enhanced citrate reabsorption via NaDC-1 up-regulation in SB rats possibly maintained plasma citrate as a result of normocitricemia (Figure 3C). A reduction in renal citrate excretion might benefit SB rats by restoring the plasma level of citrate for energy utilization. However, this might induce hypocitraturia (Figure 4D) and weaken the intrarenal defenses against CaOx crystal formation, especially when facing hyperoxlauria.

To consider the underlying mechanism for NaDC-1 upregulation-induced hypocitraturia, our results showed a parallel increase in plasma PTH and renal NaDC-1 expression in the SB rats (Figures 3D and 6C). The reduction in renal citrate clearance by PTH was postulated to increase tubular reabsorption via the effect of citrate transporters [22]. In this study, we also confirmed a direct effect of PTH on the NaDC-1 expression in the PTH receptor-expressed tubular cells, NRK-52E [17], as that recombinant PTH significantly increased the NaDC-1 expression (Figure 7D). The underlying signal pathway was dependent on PKA activation as PKA inhibition abrogated the PTH-mediated NaDC-1 up-regulation (Figure 7F). According to our knowledge, this was not known before. We concluded that hypocalcemia in our SB rats stimulated citricemic hormone PTH secretion, which increased the plasma levels of Ca^{2+} and citrate, but only citrate returned to the normocitricemic level.

PTH affected the NaDC-1 expression, and we also found that hyperoxaluria in rats or a direct oxalate treatment in tubular cells also increased the NaDC-1 expression (Figures 6C and 7D). A previous study showed that chronic metabolic acidosis led to an increase in rat renal cortical NaDC-1 mRNA and protein expression in the apical membrane of proximal tubules [26]. Acidosis directly increased NaDC-1 activity and induced hypocitraturia [27]. As low urinary pH was found in the EG-treated rats (Figure 4A), we speculated that the metabolic acidosis seen in hyperoxaluric kidneys may account for NaDC-1 up-regulation. Oxalate might also induce intracellular acidosis in tubular cells and this likely enhanced the NaDC-1 expression. Considering the effect of PTH together with oxalate (or hyperoxaluria), our results showed that there was no additive effect of acidosis and PTH on NaDC-1 up-regulation. We speculated that *in vivo* hyperoxaluria or *in vitro* oxalate possibly shares similar signal pathways, such as PKA activation after PTH treatment.

EG is known to be oxidized to oxalate by the liver and eliminated from circulation by intestinal secretions and urinary excretions [28]. SB might decrease the intestinal permeability of EG and further reduce its efficacy for hepatic oxalogenesis. However, the hyperoxaluria seen in the SB+EG group was more severe than that in the EG group (Figure

Clinical Science (2020) **134** 2565–2580
https://doi.org/10.1042/CS20200973

4C); this indicated that a shorter length of intestines in SB rats did not affect the EG absorption in the remaining intestinal tissues (duodenum and colon) for hyperoxaluric induction. For intestinal oxalate elimination, our results showed that the oxalate secretion protein Slc26a6, but not Slc26a2, was up-regulated in SB intestines (Figure 6D,E). This likely enhanced the intestinal elimination of oxalate via Slc26a6 in SB rats and prevented hyperoxalemia caused by EG absorption. A previous study showed that SB rats fed with a normal diet for 8 weeks demonstrated more urinary oxalate excretion [14]. Contrary, our SB rats without EG treatment showed no hyperoxaluria. The shorter induction time (4 weeks) likely limited spontaneous hyperoxaluric formation in our SB rats. Intestinal Slc26a6 and Slc26a2 expressions in the SB+EG group were similar to those in the control group (Figure 6D,E). This largely limited the intestinal oxalate elimination of SB rats in response to EG-induced oxalogenesis. The unchanged intestinal Slc26a6 expression in the SB+EG rats was consistent with the previous findings. They showed that Slc26a6 expression in the intestinal or colon segments was not changed in the mini-gastric bypass rats fed with a high fat and high oxalate diet to induce hyperoxaluria [29].

These results clearly indicated that there was a renal effect for the compensatory elimination of plasma oxalate if there was a deficiency in the intestinal oxalate secretions. Increased renal Slc26a6 expression contributes to hyperoxaluria [30]. Our results showed consistent results for a significant increase in Slc26a6 expression not only in the EG kidneys but also in the SB+EG kidneys (Figure 6A). A slight elevation in the Slc26a2 expression in the SB+EG kidneys when compared with the control kidneys might also contribute to hyperoxaluria (Figure 6B). Together with hypocitraturia, severe hyperoxaluria increased the degree of supersaturation in SB+EG group for CaOx formation and deposition (Figures 4E and 5). A previous study in the SB patients revealed urinary CaOx supersaturation and CaOx plugs present in the renal inner medullary collecting ducts [31]. Compared with the present study, the rat animal model showed a dispersed distribution of CaOx crystals in the SB+EG kidneys with an increase in the number, which led to tubular obstruction and dilation (Figure 5). Therefore, post-obstruction in the hyperoxaluric SB kidneys might impair renal function and lead to end-stage kidney disease [32].

In conclusion, SB aggravated hyperoxaluria-induced renal tubular damage and CaOx crystal formation through hypocitraturia. The underlying mechanism of hypocitraturia was dependent on the enhanced effects of PTH. Increased PTH levels from SB directly increased citrate transporter NaDC-1 expression via the PKA pathway in tubular cells. Together with the effect of hyperoxaluria or oxalate on the increased Slc26a6 expression, hypocitraturia worsened CaOx crystal formation in SB through poor anticrystallization against hyperoxaluria.

Limitation

The present study induces SB for 35 days only, and this induction time was shorter than clinical presentation in the resected patients who developed oxalate nephropathy. Severe hyperoxaluria in our SB rats was induced by feeding the rats with an oxalogenic diet; this was not a spontaneous formation in terms of the disease progression in SB patients. However, our animal model shared some important features similar to SB patients, such as hypocalcemia, hypocalciuria, hypocitraturia, and hyperoxaluria [33]. This study only focused on changes related to secondary parathyroidism in our experimental models. Other hormones related to the maintenance of plasma Ca^{2+} levels, such as calcitriol and calcitonin might have an influence on CaOx crystal formation caused by SB. Further study is required to examine the mechanisms in more detail regarding the hormonal effects on the SB kidneys.

Clinical perspectives

- SB increased the risk of kidney stones.
- The present study showed that SB-mediated Slc26a6 and NaDC-1 up-regulation, which aggravated oxalate nephropathy in rats by fostering hyperoxaluria and hypocitraturia, increasing the degree of supersaturation and CaOx crystal deposition via the PTH/PKA pathway.
- Our results provide novel insights into the intrarenal mechanism of SB patients associated with kidney stones and evidence regarding how PTH affects the citrate transporter.

Competing Interests

The authors declare that there are no competing interests associated with the manuscript.

Funding

This work was supported by the Far Eastern Memorial Hospital [grant numbers FEMH-2018-C-046, 105-FEMH-FJU-04 (to Yi-Shiou Tseng and Ming-Chieh Ma)]; and the Ministry of Science and Technology, Taiwan [grant number 108-2314-B-030-004-MY3 (to Ming-Chieh Ma)].

Author Contribution

Yi-Shiou Tseng and Ming-Chieh Ma conceived and designed the research plan. Yi-Shiou Tseng, Wen-Bin Wu, Yun Chen, Feili Lo Yang, and Ming-Chieh Ma performed the experiments and analyzed the data. Yi-Shiou Tseng, Wen-Bin Wu, Feili Lo Yang, and Ming-Chieh Ma interpreted the results. Yi-Shiou Tseng and Ming-Chieh Ma drafted the manuscript, with editing and revisions from Wen-Bin Wu and Yun Chen. All authors approved the final version of the manuscript.

Abbreviations

AP(CaOx) index, ion activity product of calcium oxalate; CaOx, calcium oxalate; Ccr, creatinine clearance; EG, ethylene glycol; LDH, lactate dehydrogenase; MTT, 3-(4,5-dimethylthiazol-2-yl)-2,5-diphenyltetrazolium bromide; NaDC-1, sodium-dependent dicarboxylate cotransporter-1; Oxa, oxalate; PBS, phosphate buffered saline; PKA, protein kinase A; PTH, parathyroid hormone; SB, short bowel; Slc26a2/6, solute carrier family 26 member 2 or 6.

References

1 Bambach, C.P., Robertson, W.G., Peacock, M. and Hill, G.L. (1981) Effect of intestinal surgery on the risk of urinary stone formation. *Gut* **22**, 257–263, https://doi.org/10.1136/gut.22.4.257
2 Parks, J.H., Worcester, E.M., Corey O'Connor, R. and Coe, F.L. (2003) Urine stone risk factors in nephrolithiasis patients with and without bowel disease. *Kidney Int.* **63**, 255–265, https://doi.org/10.1046/j.1523-1755.2003.00725.x
3 Jiang, Z., Aronson, P.S., Ko, N., Knauf, F., Robertson, W.G., Anderson, J.M. et al. (2011) Net intestinal transport of oxalate reflects passive absorption and SLC26A6-mediated secretion. *J. Am. Soc. Nephrol.* **22**, 2247–2255
4 Alper, S.L., Karniski, L.P., Akhavein, A., Heneghan, J.F., Vandorpe, D.H., Salas, M.J. et al. (2010) Regulated transport of sulfate and oxalate by SLC26A2/DTDST. *Am. J. Physiol. Cell Physiol.* **298**, C1363–C1375
5 Porter, J.L., Hofmann, A.F., Guirl, M.J., Neimark, S., Santa Ana, C.A., Fordtran, J.S. et al. (2002) Conjugated bile acid replacement therapy reduces urinary oxalate excretion in short bowel syndrome. *Am. J. Kidney Dis.* **41**, 230–237
6 Seetharam, P. and Rodrigues, G. (2011) Short bowel syndrome: a review of management options. *Saudi J. Gastroenterol.* **17**, 229–235
7 Thamilselvan, V., Menon, M. and Thamilselvan, S. (2009) Oxalate-induced activation of PKC-α and -δ regulates NADPH oxidase-mediated oxidative injury in renal tubular epithelial cells. *Am. J. Physiol. Renal Physiol.* **297**, F1399–F1410, https://doi.org/10.1152/ajprenal.00051.2009
8 Antinozzi, P.A., Brown, C.M. and Purich, D.L. (1992) Calcium oxalate monohydrate crystallization: citrate inhibition of nucleation and growth steps. *J. Cryst. Growth* **125**, 215–222, https://doi.org/10.1016/0022-0248(92)90335-G
9 El-Shall, H., Jeon, J.H., Abdel-Aal, E.A., Khan, S., Gower, L. and Rabinovich, Y. (2004) A study of primary nucleation of calcium oxalate monohydrate: II. Effect of urinary species. *Cryst. Res. Technol.* **39**, 222–229, https://doi.org/10.1002/crat.200310227
10 Sheng, X., Jung, T., Wesson, J.A. and Ward, M.D. (2005) From The Cover: Adhesion at calcium oxalate crystal surfaces and the effect of urinary constituents. *Proc. Natl. Acad. Sci. U.S.A.* **102**, 267–272, https://doi.org/10.1073/pnas.0406835101
11 Pajor, A.M. (2006) Molecular properties of the SLC13 family of dicarboxylate and sulfate transporters. *Pflugers Arch.* **451**, 597–605, https://doi.org/10.1007/s00424-005-1487-2
12 Huang, H.S. and Ma, M.C. (2015) High sodium-induced oxidative stress and poor anticrystallization defense aggravate calcium oxalate crystal formation in rat hyperoxaluric kidneys. *PLoS ONE* **10**, 1–19
13 Ohana, E., Shcheynikov, N., Moe, O.W. and Muallem, S. (2013) SLC26A6 and NaDC-1 transporters interact to regulate oxalate and citrate homeostasis. *J. Am. Soc. Nephrol.* **24**, 1617–1626, https://doi.org/10.1681/ASN.2013010080
14 Worcester, E.M., Chuang, M., Laven, B., Orvieto, M., Coe, F.L., Evan, A.P. et al. (2005) A new animal model of hyperoxaluria and nephrolithiasis in rats with small bowel resection. *Urol. Res.* **33**, 380–382, https://doi.org/10.1007/s00240-005-0489-z
15 Tiselius, H.-G., Ferraz, R.R.N. and Heilberg, I.P. (2003) An approximate estimate of the ion-activity product of calcium oxalate in rat urine. *Urol. Res.* **31**, 410–413, https://doi.org/10.1007/s00240-003-0363-9
16 Pizzolato, P. (1964) Histochemical recognition of calcium oxalate. *J. Histochem. Cytochem.* **12**, 333–336, https://doi.org/10.1177/12.5.333
17 Santos, S., Bosch, R.J., Ortega, A., Largo, R., Fernández-Agulló, T., Gazapo, R. et al. (2001) Up-regulation of parathyroid hormone-related protein in folic acid-induced acute renal failure. *Kidney Int.* **60**, 982–995, https://doi.org/10.1046/j.1523-1755.2001.060003982.x
18 Lu, C.L., Liao, C.H., Lu, K.C. and Ma, M.C. (2020) TRPV1 hyperfunction involved in uremic toxin indoxyl sulfate-mediated renal tubular damage. *Int. J. Mol. Sci.* **21**, E6212, https://doi.org/10.3390/ijms21176212
19 Bastepe, M., Turan, S., He, Q., Hospital, M.G. and Medical, H. (2018) G proteins in the control of parathyroid hormone actions. *J. Mol. Endocrinol.* **58**, 1–35
20 Haderslev, K.V., Jeppesen, P.B., Mortensen, P.B. and Staun, M. (2000) Absorption of calcium and magnesium in patients with intestinal resections treated with medium chain fatty acids. *Gut* **46**, 819–823, https://doi.org/10.1136/gut.46.6.819
21 Evenepoel, P., Bover, J. and Ureña Torres, P. (2016) Parathyroid hormone metabolism and signaling in health and chronic kidney disease. *Kidney Int.* **90**, 1184–1190, https://doi.org/10.1016/j.kint.2016.06.041

Clinical Science (2020) **134** 2565–2580
https://doi.org/10.1042/CS20200973

22 Costello, L.C. and Franklin, R.B. (2016) Plasma citrate homeostasis: how it is regulated; and its physiological and clinical implications. An important, but neglected, relationship in medicine. *HSOA J. Human Endocrinol.* **1**, 005
23 Worcester, E.M. (2002) Stones from bowel disease. *Endocrinol. Metab. Clin. North Am.* **31**, 979–999, https://doi.org/10.1016/S0889-8529(02)00035-X
24 Martínez-Reyes, I. and Chandel, N.S. (2020) Mitochondrial TCA cycle metabolites control physiology and disease. *Nat. Commun.* **11**, 1–11, https://doi.org/10.1038/s41467-019-13668-3
25 Kelly, D.G., Tappenden, K.A. and Winkler, M.F. (2014) Short bowel syndrome: highlights of patient management, quality of life, and survival. *JPEN J. Parenter. Enteral Nutr.* **38**, 427–437, https://doi.org/10.1177/0148607113512678
26 Aruga, S., Wehrli, S., Kaissling, B., Moe, O.W., Preisig, P.A., Pajor, A.M. et al. (2000) Chronic metabolic acidosis increases NaDC-1 mRNA and protein abundance in rat kidney. *Kidney Int.* **58**, 206–215, https://doi.org/10.1046/j.1523-1755.2000.00155.x
27 Zuckerman, J.M. and Assimos, D.G. (2009) Hypocitraturia: pathophysiology and medical management. *Rev. Urol.* **11**, 134–144
28 Scalley, R.D., Ferguson, D.R., Piccaro, J.C., Smart, M.L. and Archie, T.E. (2002) Treatment of ethylene glycol poisoning. *Am. Fam. Phys.* **66**, 807–812
29 Ormanji, M.S., Korkes, F., Meca, R., Ishiy, C.S.R.A., Finotti, G.H.C., Ferraz, R.R.N. et al. (2017) Hyperoxaluria in a model of mini-gastric bypass surgery in rats. *Obes. Surg.* **27**, 3202–3208
30 Wang, S., Pokhrel, G., Wang, T., Yin, C., Jiang, H., Chen, Y. et al. (2018) High expression of SLC26A6 in the kidney may contribute to renal calcification via an SLC26A6-dependent mechanism. *PeerJ* **6**, e5192
31 Evan, A.P., Lingeman, J.E., Worcester, E.M., Bledsoe, S.B., Sommer, A.J., Williams, J.C. et al. (2010) Renal histopathology and crystal deposits in patients with small bowel resection and calcium oxalate stone disease. *Kidney Int.* **78**, 310–317, https://doi.org/10.1038/ki.2010.131
32 Nazzal, L., Puri, S. and Goldfarb, D.S. (2016) Enteric hyperoxaluria: an important cause of end-stage kidney disease. *Nephrol. Dialysis Transplant.* **31**, 375–382, https://doi.org/10.1093/ndt/gfv005
33 Johnson, E., Vu, L. and Matarese, L.E. (2018) Bacteria, bones, and stones: managing complications of short bowel syndrome. *Nutr. Clin. Pract.* **33**, 454–466, https://doi.org/10.1002/ncp.10113